Nucleons or diquarks? Competition between clustering and color superconductivity in quark matter

Stéphane Pepin*, Michael C. Birse and Judith A. McGovern

Theoretical Physics Group, Department of Physics and Astronomy, University of Manchester, Manchester M13 9PL, United Kingdom

Niels R. Walet

Department of Physics, UMIST, P.O. Box 88, Manchester M60 1QD, United Kingdom

(February 1, 2008)

Abstract

We study the instabilities of quark matter in the framework of a generalized Nambu–Jona-Lasinio model, in order to explore possible competition between three-quark clustering to form nucleons and diquark formation leading to color superconductivity. Nucleon and Δ solutions are obtained for the relativistic Faddeev equation at finite density and their binding energies are compared with those for the scalar and axial-vector diquarks found from the Bethe-Salpeter equation. In a model with interactions in both scalar and axial diquark channels, bound nucleons exist up to nuclear matter density. However, except at densities below about a quarter of that of nuclear matter, we find that scalar diquark formation is energetically favored. This raises the question of whether a realistic phase diagram of baryonic matter can be obtained from any model which does not incorporate color confinement.

*Current address: Max-Planck Institut für Kernphysik, Postfach 103980, D-69029 Heidelberg, Germany

I. INTRODUCTION

In contrast to QCD at finite temperature, rather little is known about QCD at finite density. Technical difficulties (such as the complex fermionic determinant at finite chemical potential) make lattice Monte-Carlo simulations very difficult. Even though some techniques are being developed to overcome these problems (for example, the Glasgow method [1] or the technique of imaginary chemical potential [2]), they are not yet able to provide unambiguous results.

However, models of QCD seem to indicate a rich phase structure in high-density quark matter. In particular, much attention has recently been devoted to so-called "color superconductivity" [3,4]: an arbitrarily weak attractive force makes the Fermi sea of quarks unstable at high density with respect to diquark formation and induces Cooper pairing (diquark condensation). Although this phenomenon had been studied earlier [5,6,8], the large magnitude of the superconducting gap found in the more recent studies [3,4] (more than 100 MeV) suggested that this was much more important than had been thought previously and has generated an extensive literature. In Refs. [3,4] an instanton model was used to calculate the gap at finite density and zero temperature. Berges and Rajagopal [7] extended this work and calculated the phase diagram of strongly interacting matter as a function of temperature and baryon-number density in the same model. Identical results were found in the Nambu–Jona-Lasinio model [9]. The existence of such a color-superconducting gap could have important consequences for the physics of neutron stars or even for heavy ion collisions [10,11]. (For a review of the field, see: [12].)

Previous studies of color superconductivity have focused on instabilities of the quark Fermi sea with respect to diquarks only. Of course, it is known that at lower densities (of the order of nuclear matter density) three-quark clusters—nucleons—are the dominant degrees of freedom. Here we address the question of the possibility of a competition between diquark condensation and three-quark clustering at finite density. To answer such a question fully would require a three-particle generalization of the BCS treatment, a complicated task.

As a first step towards this goal, we look for instabilities of the quark Fermi sea with respect to three-quark clustering by studying the nucleon binding energy in quark matter with finite density. A bound nucleon at finite density would be a signal of instability with respect to clustering (in the same way that a bound diquark at finite density is a signal of instability with respect to diquark condensation). A comparison of the magnitudes of the binding energies of the diquark and the nucleon can give some idea of the relevance of these degrees of freedom. Very recently, Beyer *et al.* have studied a similar clustering problem for three nucleons in nuclear matter [13].

To perform this study we solve the Bethe-Salpeter equation for the diquarks and the Faddeev equation for the nucleon (and also, for completeness, for the Δ) within the framework of a Nambu–Jona-Lasinio (NJL) model. The use of a separable interaction simplifies the treatment of the Faddeev equation considerably. The form of the equation reduces to that of a Bethe-Salpeter equation describing the interaction between a quark and a diquark. At zero density, several groups have used this Faddeev approach to study baryons in the NJL model (for example, Refs. [14–19]). More recent papers [20] have extended this treatment to incorporate a mechanism for confinement. In this work we will mainly follow the formalism developed by Ishii, Bentz and Yazaki [18], generalizing it to finite density. In this type of approach, it is crucial to include the axial-vector diquark channel in addition to the scalar channel, as otherwise the nucleon is very weakly bound. In previous preliminary studies, keeping only the scalar channel, we have found that binding of a nucleon in matter is only possible at very low densities, less than 10% of nuclear matter density [21].

The paper is organized as follows: in the next section, we briefly describe the NJL model and its application to quark-quark interaction. The parameters used in our study are also discussed. In Sec. 3 the Bethe-Salpeter equations in the scalar and axial-vector diquark channels are solved. The form of the Faddeev equation for the nucleon is presented in Sec. 4. In Sec. 5, we describe the numerical techniques used and in Sec. 6 we present our results for the nucleon and the Δ at finite density. Finally, we draw some conclusions in Sec. 7.

II. THE MODEL

The NJL model provides a simple implementation of dynamically broken chiral symmetry, based on a two-body contact interaction [22]. In spite of the fact that the model does not incorporate confinement, it has been successfully applied to the description of mesonic properties at low energy. (For reviews, see Refs. [23,24].)

The model Lagrangian has the form

$$\mathcal{L} = \overline{\psi}(i\partial\!\!\!/ - m)\psi + \mathcal{L}_I, \tag{1}$$

where $\mathcal{L}_I$ is the interaction Lagrangian. In the present work we consider only the chiral limit, setting the current quark mass m to zero. Several versions of the NJL interaction can be found in the literature. The original version [22] is

$$\mathcal{L}_I = g\Big[(\overline{\psi}\psi)^2 + (\overline{\psi}i\gamma_5\vec{\tau}\psi)^2\Big]. \tag{2}$$

One can also work with a color-current interaction,

$$\mathcal{L}_I = -g\sum_c \left(\overline{\psi}\gamma_\mu \tfrac{1}{2}\lambda_c\psi\right)^2, \tag{3}$$

where λ_c ($c = 1, ..., 8$) are the usual Gell-Mann matrices.

Whatever version of the model is chosen, a Fierz transformation should be performed in order to antisymmetrize the interaction Lagrangian. This allows $\mathcal{L}_I$ to be brought into a form where the interaction strength in a particular channel can be read off directly from its coefficient in the Lagrangian. For the $q\overline{q}$ channel, one just rewrites $\mathcal{L}_I$ into the form $\mathcal{L}_{I,q\overline{q}} = \frac{1}{2}(\mathcal{L}_I + \mathcal{L}_{I,F})$ where $\mathcal{L}_{I,F}$ is the Fierz transformed form of $\mathcal{L}_I$. We shall need here only the scalar and pseudoscalar terms of the $q\overline{q}$ interaction. These have the same form as Eq. (2), but with a coupling constant g_π which is related to the original coupling constant g of the Lagrangian by a coefficient given by the Fierz transformation. For example, one has $g_\pi/g = 13/12$ for the model defined by Eq. (2) and $g_\pi/g = -2/9$ for Eq. (3).

To study the nucleon we also need to rewrite the interaction Lagrangian in the form of a qq interaction. This is done by a Fierz transformation to the qq channels, which allows

the interaction to be expressed as a sum of terms of the form $(\overline{\psi}A\overline{\psi}^T)(\psi^T B\psi)$, where the matrices A and B are overall antisymmetric in Dirac, isospin and color indices. (We use the Dirac representation for the γ-matrices and follow the conventions of Itzykson and Zuber [25].)

As our three-quark state must be a color singlet, the diquark channels of interest are color anti-triplet. For a local interaction the relevant channels are the scalar $(0^+, T = 0)$ and axial-vector $(1^+, T = 1)$ ones. These are also the channels in which more realistic interactions (including, for example, one-gluon exchange) are expected to be most attractive. Explicitly, we have

$$\mathcal{L}_S = g_S \sum_a \left(\bar{\psi}\gamma_5 C\tau_2\beta^a\bar{\psi}^T\right)\left(\psi^T C^{-1}\gamma_5\tau_2\beta^a\psi\right), \tag{4}$$

for the scalar channel and

$$\mathcal{L}_A = g_A \sum_{i,a} \left(\bar{\psi}\gamma_\mu C\tau_i\tau_2\beta^a\bar{\psi}^T\right)\left(\psi^T C^{-1}\gamma^\mu\tau_2\tau_i\beta^a\psi\right), \tag{5}$$

for the axial-vector one. The matrices $\beta^a = \sqrt{\frac{3}{2}}\,\lambda^a$ for $a = 2, 5, 7$ project onto the color $\bar{3}$ channel and $C = i\gamma_2\gamma_0$ is the charge conjugation matrix. The coupling strengths g_S and g_A are again related to the original g by a coefficient given by the Fierz transformation. In the following we do not choose a specific version of the NJL Lagrangian but instead treat the physical couplings g_π, g_S, g_A as independent parameters.

The gap equation for the constituent quark mass M reads

$$M = 2ig_\pi \int \frac{d^4k}{(2\pi)^4}\mathrm{Tr}[S(k)], \tag{6}$$

where the quark propagator is

$$S(k) = \frac{1}{\not{k} - M + i\epsilon}. \tag{7}$$

The integral (6) diverges and so has to be regularized. There are various regularization schemes at our disposal: Pauli-Villars, proper-time, and 3- or 4-momentum cut-off. In this work we use a sharp cut-off Λ on the 3-momentum to regularize the loop integrals, since

TABLE I. Values of the parameters g_π and Λ for the two values we use for the constituent quark mass M. For each M, the qq coupling ratios g_S/g_π and g_A/g_π are determined by fitting the N and Δ masses. In each case we also list, in parentheses, the minimal value of the coupling ratio required to produce bound diquarks.

M (GeV)	g_π (GeV^{-2})	Λ (GeV)	g_S/g_π (min.)	g_A/g_π (min.)
0.45	7.914	0.579	0.72 (0.33)	0.46 (0.37)
0.5	8.634	0.573	0.72 (0.28)	0.53 (0.31)

this is conveniently applied to systems of finite density. Although a 3-momentum cut-off is not Lorentz invariant, this is less relevant at finite density where there is a much larger, physical, breaking of Lorentz invariance due to the presence of a quark Fermi sea. In any case, we shall show that physical observables depend only weakly on the choice of regulator.

The two parameters g_π and Λ can be fitted to a given value of the constituent quark mass and to the pion decay constant $f_\pi = 93$ MeV. This last quantity is evaluated from

$$f_\pi^2 = -12iM^2 \int \frac{d^4k}{(2\pi)^4} \frac{1}{(p^2 - M^2)^2}. \tag{8}$$

In the following calculations we use two different values for the constituent mass $M = 450$ MeV and $M = 500$ MeV, both of which have been chosen to be large enough that the mass of the Δ lies below the three-quark threshold. In Table I we list the values of g_π and Λ for the corresponding constituent masses. As one can see, the values for the cut-off are relatively low and decrease with increasing constituent mass. One cannot push the constituent mass to higher values as otherwise the cut-off would approach (or, worse, become smaller than) the quark mass.

The effects of finite density on the constituent mass are taken into account by introducing the Fermi momentum k_F as a lower cut-off on the integral in the gap equation (6). In Figure 1 we show the evolution of the constituent mass as a function of the Fermi momentum for

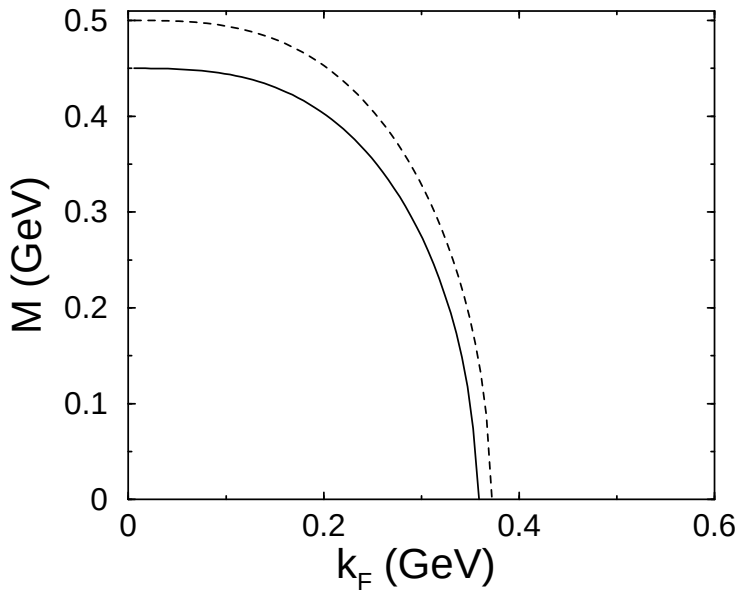

FIG. 1. Evolution of the constituent quark mass M with the Fermi momentum k_F for $M(k_F = 0) = 450$ MeV (continuous curve) and $M(k_F = 0) = 500$ MeV (dashed).

the two sets of parameters corresponding to $M = 450$ and 500 MeV. For these parameters, the restoration of chiral symmetry occurs at $k_F = 359$ MeV and $k_F = 372$ MeV respectively. (For comparison, nuclear matter density corresponds to a quark Fermi momentum of $k_F = [\frac{3}{2}\pi^2\rho_B]^{1/3} = 270$ MeV).

III. THE TWO-BODY T-MATRIX

The diquark T-matrix is an essential building block for the Faddeev equation. It is obtained by solving the Bethe-Salpeter equation in the ladder approximation,

$$T^{\alpha\beta,\gamma\delta}(k) = K^{\alpha\beta,\gamma\delta} + \frac{1}{2}\sum_{\lambda,\epsilon,\lambda',\epsilon'}\int \frac{d^4q}{(2\pi)^4} K^{\alpha\beta,\lambda\epsilon} S^{\lambda\lambda'}(k+q) S^{\epsilon\epsilon'}(-q) T^{\lambda'\epsilon',\gamma\delta}(k). \tag{9}$$

In the scalar diquark channel, the interaction kernel K is

$$K_S^{\alpha\beta,\gamma\delta} = 4ig_S \sum_a (\gamma_5 C\tau_2\beta^a)^{\alpha\beta}(C^{-1}\gamma_5\tau_2\beta^a)^{\gamma\delta}. \tag{10}$$

This interaction is momentum-independent and so Eq. (9) can be solved easily to get the diquark T-matrix in the scalar channel [18]:

$$T_S^{\alpha\beta,\gamma\delta}(k) = \sum_a (\gamma_5 C\tau_2\beta^a)^{\alpha\beta}\bar{\tau}_S(k)(C^{-1}\gamma_5\tau_2\beta^a)^{\gamma\delta}, \tag{11}$$

with

$$\bar{\tau}_S(k) = \frac{4ig_S}{1+2g_S\Pi_S(k^2)}, \tag{12}$$

and

$$\Pi_S(k^2) = 6i\int\frac{d^4q}{(2\pi)^4}\mathrm{Tr}_D[\gamma_5 S(q)\gamma_5 S(k+q)]. \tag{13}$$

If the T-matrix (12) has a pole, this gives us the mass of the bound scalar diquark. Note that, if one replaces the coupling g_S by g_π, the denominator of (12) is the same as that in the pion $q\overline{q}$ channel [18]. This means that for $g_S = g_\pi$ the scalar diquark and pion are degenerate, and have zero mass in the chiral limit. Since diquarks do not condense in the vacuum, this puts an upper limit to the choice of the scalar coupling g_S.

In the axial-vector channel, the kernel is

$$K_A^{\alpha\beta,\gamma\delta} = 4ig_A\sum_{a,i}(\gamma_\mu C\tau_i\tau_2\beta^a)^{\alpha\beta}(C^{-1}\gamma^\mu\tau_2\tau_i\beta^a)^{\gamma\delta}, \tag{14}$$

and the solution of (9) can be shown to be

$$T_A^{\alpha\beta,\gamma\delta}(k) = \sum_{a,i}(\gamma_\mu C\tau_i\tau_2\beta^a)^{\alpha\beta}\bar{\tau}_A^{\mu\nu}(k)(C^{-1}\gamma_\nu\tau_2\tau_i\beta^a)^{\gamma\delta}, \tag{15}$$

with

$$\bar{\tau}_a^{\mu\nu}(k) = 4ig_A\left[\frac{g^{\mu\nu}-k^\mu k^\nu/k^2}{1+2g_A\Pi_{A,T}(k^2)} + \frac{k^\mu k^\nu/k^2}{1+2g_A\Pi_{A,L}(k^2)}\right]. \tag{16}$$

Here, the axial polarization tensor,

$$\Pi_A^{\mu\nu}(k) = 6i\int\frac{d^4q}{(2\pi)^4}\mathrm{Tr}_D[\gamma^\mu S(q)\gamma^\nu S(k+q)], \tag{17}$$

has been decomposed in the form

$$\Pi_A^{\mu\nu}(k) = \Pi_{A,T}(k^2)\left(g^{\mu\nu}-\frac{k^\mu k^\nu}{k^2}\right) + \Pi_{A,L}(k^2)\frac{k^\mu k^\nu}{k^2}. \tag{18}$$

Again, a bound axial-vector diquark corresponds to a pole in the T-matrix (16). The minimum values of the coupling ratios g_S/g_π and g_A/g_π required to get bound diquarks at zero density can be found in Table I.

Note that when the loop integrals are regulated with a simple cut-off on either the 3- or 4-momentum, the longitudinal polarizability in this channel, $\Pi_{A,L}(k^2)$ does not vanish, in contrast to the hybrid method involving dimensional regularization used by Ishii *et al.* [18,26]. However, since there is no conserved current coupled to these states, this does not violate any physical symmetries.

In the presence of quark matter, manifest Lorentz invariance is broken and the structure of the polarization tensor $\Pi_A^{\mu\nu}(k)$ becomes more complicated. For a diquark momentum in the z-direction, $k = (k^0, 0, 0, k^3)$, it can be written

$$\Pi_A^{\mu\nu}(k^0, k^3) = \begin{pmatrix} A & 0 & 0 & Dk^0k^3 \\ 0 & B & 0 & 0 \\ 0 & 0 & B & 0 \\ Dk^0k^3 & 0 & 0 & B + C(k^3)^2 \end{pmatrix}. \tag{19}$$

The use of a 3-momentum cut-off does lead to deviations from the Lorentz covariant structure shown in (18) even in the vacuum case, but we have checked that these are small.

The results for diquarks at zero density are qualitatively similar to those in Ref. [18] despite a different choice of regulator and the use of a nonzero current-quark mass in that work. For a constituent quark mass of $M = 400$ MeV, as used in that work, we find that the minimum value of g_S/g_π for diquark binding is 0.4 compared with 0.33 in Ref. [18]. For $g_S/g_\pi = 0.6$ and $g_S/g_\pi = 0.8$ we get scalar diquark masses of 699 and 507 MeV respectively, compared with 627 and 446 MeV (cf. Table 2 of Ref. [18]). To bind the axial-vector diquark, we find a minimum coupling strength $g_A/g_\pi = 0.46$. The corresponding value given in Ref. [18] is 2.0, but this should in fact be divided by a factor of 4 [26], and so we again have qualitative agreement with that work.

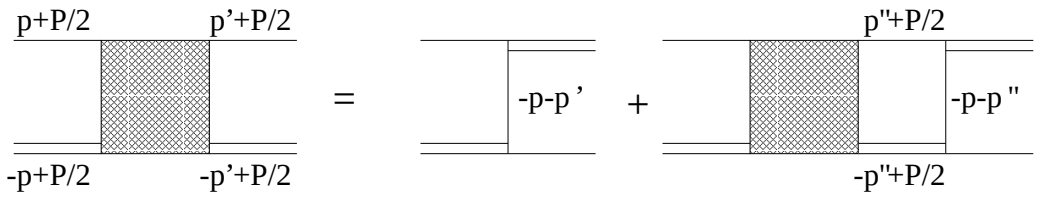

FIG. 2. Diagrammatic representation of the Faddeev equation (20).

IV. THE FADDEEV EQUATION

Because of the separability of the NJL interaction, the ladder approximation to the Faddeev equation for the three-body system can be reduced to an effective two-body Bethe-Salpeter equation. This can be thought of as describing the interaction between a quark and a diquark, although it is not necessary that the diquark be bound. In our derivation of this equation, we have followed the procedure described in [18]. We reproduce here only the main steps of this derivation; the details can be found in the original papers [15,18]. In the case of a purely scalar qq interaction, a thorough discussion of the Faddeev equation can also be found in Ref. [17].

We denote the scattering amplitude of a quark on a diquark by $X^{\alpha\beta}_{ab}$. The indices a, b label the diquark and, following the convention of Ref. [18] they take the values 5 (for the scalar diquark) and 0, 3, +1 and −1 (for the components of the axial-vector diquark in a spherical basis). These diquark indices will be written as subscripts or superscripts to indicate that the components of the axial diquark are covariant or contravariant respectively. The Dirac indices α, β label the quark, taking the values 1 to 4. The amplitude obeys the integral equation,

$$X^{\alpha\beta}_{ab}(p',p) = Z^{\alpha\beta}_{ab}(p',p) + \sum_{\gamma,c,\delta,d} \int \frac{d^4p''}{(2\pi)^4} Z^{\alpha\gamma}_{ac}(p',p'') S^{\gamma\delta}(P/2+p'') \bar{\tau}^{cd}(P/2-p'') X^{\delta\beta}_{db}(p'',p), \tag{20}$$

corresponding to the diagram shown in Fig. 2. The piece of the kernel containing the propagator of the exchanged quark is

$$Z^{\alpha\beta}_{ab}(p',p) = \sum_{\gamma,\delta} \Omega^{\alpha\delta}_{b} S^{\gamma\delta}(-p-p') \bar{\Omega}^{\gamma\beta}_{a}, \tag{21}$$

where Ω and $\bar{\Omega}$ are the two-body vertex functions, already used in Eqs. (10) and (14). The propagator of the spectator quark is $S(P/2+p'')$, and $\bar{\tau}^{cd}(P/2-p'')$ is the two-body amplitude for the two interacting quarks. The separable nature of the two-body interaction means that this amplitude can be thought of as a diquark propagator, but one should remember that it describes the propagation of all two-quark states, not just the bound states (if they exist). It can be written as

$$\bar{\tau}^{cd} = \begin{pmatrix} \bar{\tau}_S & 0 \\ 0 & \bar{\tau}_A^{\mu\mu'} \end{pmatrix}. \tag{22}$$

where $\bar{\tau}_S$ and $\bar{\tau}_A^{\mu\mu'}$ are the scalar and axial-vector diquark "propagators" given by Eqs. (12) and (16) respectively.

To find bound states of the three-body system, we solve the homogeneous version of equation (20) for the effective two-body vertex function of a quark and a diquark. This vertex function, X_a^α, is related to the amplitude $X_{ab}^{\alpha\beta}$ by

$$X_{ab}^{\alpha\beta}(p',p) \to \frac{X_a^\alpha(p')\bar{X}_b^\beta(p)}{P^2 - M_B^2 + i\epsilon}, \qquad \text{as} \qquad P^2 \to M_B^2, \tag{23}$$

where M_B is the mass of the bound baryon. From (20) one obtains the equation

$$X_a^\alpha(p) = \sum_{\gamma,c,\delta,d} \int \frac{d^4p'}{(2\pi)^4} Z_{ac}^{\alpha\gamma}(p,p') S^{\gamma\delta}(P/2+p') \bar{\tau}^{cd}(P/2-p') X_d^\delta(p'), \tag{24}$$

for the vertex function.

This equation needs to be projected onto states of definite color, spin and isospin. Projecting the kernel $Z_{ac}^{\alpha\gamma}$ onto a color-singlet state gives

$$Z_{ac}^{\alpha\gamma}(p,p') = -3 \begin{pmatrix} \gamma_5 S(p+p')\gamma_5 & \sqrt{3}\gamma_\mu S(p+p')\gamma_5 \\ \sqrt{3}\gamma_5 S(p+p')\gamma_{\mu'} & -\gamma_\mu S(p+p')\gamma_{\mu'} \end{pmatrix}_{\alpha\gamma}, \tag{25}$$

for the isospin-$\frac{1}{2}$ channel, and

$$Z_{ac}^{\alpha\gamma}(p,p') = -6\Big(\gamma_\mu S(p+p')\gamma_{\mu'}\Big)_{\alpha\gamma}, \tag{26}$$

for the isospin-$\frac{3}{2}$ channel.

Next, a projection onto good spin and parity must be carried out. Like Ishii *et al.* [18] we use the helicity formalism of Jacob and Wick [28], constructing first a basis of states with definite helicity by acting with a rotation operator on helicity eigenstates whose momentum $\tilde{\mathbf{p}}$ lies along the z-axis:

$$|\mathbf{p}(\omega), \alpha, a\rangle = \mathcal{R}(\omega)|\tilde{\mathbf{p}}, \alpha, a\rangle = \sum_{\alpha', a'} S^{\alpha'\alpha}(\omega)\hat{R}^{a'}{}_{a}(\omega)|\mathbf{p}(\omega), \alpha', a'\rangle, \tag{27}$$

where $\mathbf{p}(\omega) = R(\omega)\tilde{\mathbf{p}}$ lies in a general direction given by the Euler angles ω. Both the helicity s_α and the intrinsic parity η_α of the quark state are specified by the label $\alpha = 1,\ldots,4$, with $s_{1,3} = \frac{1}{2}$, $s_{2,4} = -\frac{1}{2}$, $\eta_{1,2} = +1$ and $\eta_{3,4} = -1$. The helicity λ_a of the diquark is specified by the label a, with $\lambda_{5,0,3} = 0$, $\lambda_{+1} = +1$ and $\lambda_{-1} = -1$. The corresponding intrinsic parities are $\eta_{5,3,+1,-1} = +1$ and $\eta_0 = -1$. Note that our use of these labels differs slightly from that of Ishii *et al.* [18]. The rotation matrices appearing Eq. (27) are

$$S^{\alpha'\alpha}(\omega) = \exp\left(is_{\alpha'}\psi\right) \begin{pmatrix} d^{1/2}(\theta) & 0 \\ 0 & d^{1/2}(\theta) \end{pmatrix}_{s_{\alpha'}s_\alpha} \exp\left(is_\alpha\phi\right), \tag{28}$$

and

$$\hat{R}^{a'}_{a}(\omega) = \exp\left(i\lambda_{a'}\psi\right) \begin{pmatrix} 1 & 0 & 0 \\ 0 & 1 & 0 \\ 0 & 0 & d^{1}(\theta) \end{pmatrix}_{\lambda_{a'}\lambda_a} \exp\left(i\lambda_a\phi\right), \tag{29}$$

where the $d(\theta)$ are Wigner d-functions in Edmonds' convention [27].

These basis states must now be projected onto good angular momentum:

$$|\bar{p}, \alpha, a; JM\rangle = \sqrt{\frac{2J+1}{8\pi^2}} \int d\omega\, \mathcal{D}^{J}_{M, s_\alpha + \lambda_a}(\omega)|\mathbf{p}(\omega), \alpha, a\rangle, \tag{30}$$

where $\bar{p} = |\mathbf{p}|$. The resulting Faddeev equation for states of spin J has the form

$$X^{\alpha}_{J,a}(p_0, p) = \sum_{\beta, b} \frac{1}{(2\pi)^5} \int dp'_0\, p'^2 dp'\, F^{\alpha\beta b}_{J,a}(p_0, p, p'_0, p') X^{\beta}_{J,b}(p'_0, p'). \tag{31}$$

The expression for the kernel is given by the formula (D.9) of Ref. [18]. We reproduce its form in our notation here,

$$
\begin{aligned}
F^{\alpha'\alpha a}_{J,a'}(p'_0\bar{p}', p_0\bar{p}) = &-3C^J_{aa'}(2\pi)^2 \\
&\times \sum_{b,c} \int_0^\pi \sin\theta \, d\theta \, d^J_{s_\alpha+\lambda_a, s_{\alpha'}+\lambda_{a'}}(\theta) \\
&\quad \times \frac{1}{(p_0+p'_0)^2 - (\bar{p}^2 + \bar{p}'^2 + 2\bar{p}\bar{p}'\cos\theta) - M^2} \\
&\quad \times \Big\{ \Big[\gamma^*_{a'} \hat{d}^{1/2}(-\theta)\gamma^b \not{p} + \not{\bar{p}}' \gamma^*_{a'} \hat{d}^{1/2}(-\theta)\gamma^b \\
&\qquad -M\gamma^*_{a'}\hat{d}^{1/2}(-\theta)\gamma^b - 2\hat{d}^{1/2}(-\theta)\hat{d}^1(-\theta)_{\lambda_{a'}\lambda_b}\not{p} \\
&\qquad -2\not{\bar{p}}'\hat{d}^{1/2}(-\theta)\hat{d}^1(-\theta)_{\lambda_{a'}\lambda_b} + 2M\hat{d}^{1/2}(-\theta)\hat{d}^1(-\theta)_{\lambda_{a'}\lambda_b} \\
&\qquad +2\hat{d}^{1/2}(-\theta)\hat{d}^1(-\theta)_{\lambda_{a'}\lambda_c} p_c \gamma^b \\
&\qquad +2\gamma^*_{a'}\hat{d}^{1/2}(-\theta)\tilde{p}'^c \hat{d}^1(-\theta)_{\lambda_c\lambda_b} \Big] S(P/2+p) \Big\}_{\alpha'\alpha} \\
&\quad \times \tau^a_b(P/2-p).
\end{aligned} \tag{32}
$$

In Eq. (32), the asterisk denotes complex conjugation with respect to the explicit factor of i in the spherical-basis components of vectors only. The matrices $\hat{d}^{1/2}(\theta)$ and $\hat{d}^1(\theta)$ are the ones appearing between the phase factors in Eqs. (28) and (29) respectively. In the spin-$\frac{1}{2}$ channel, the numerical coefficients $-3C^{1/2}_{a'a}$ are the ones appearing in Eq. (25), with $C^{1/2}_{a'a}$ equal to $+1$ if both indices refer to scalar diquarks, -1 if both refer to axial diquarks, and $\sqrt{3}$ if they are mixed.

Finally the Faddeev equation has to be projected onto positive parity states. The resulting equation has the same form as (31), but with the positive-parity kernel,

$$
F^{(+)\alpha\beta b}_{J,a} = F^{\alpha\beta b}_{J,a} + z_{\beta b} F^{\alpha\bar{\beta}\bar{b}}_{J,a}, \tag{33}
$$

where the quark index $\bar{\beta}$ is defined such that $s_{\bar{\beta}} = -s_\beta$ and $\eta_{\bar{\beta}} = \eta_\beta$, and the diquark index $\bar{b}$ is defined similarly. The phase factor is

$$
z_{\beta b} = \eta_\beta \eta_b (-1)^{J-s-j_b}, \tag{34}
$$

where η_β and η_b are the intrinsic parities of the quark and diquark, and their intrinsic spins are $s = \frac{1}{2}$, $j_{5,0} = 0$ and $j_{3,+1,-1} = 1$. The parity projection cuts the set of 20 coupled equations down to 10. Of these, two describe only states with spin-$\frac{3}{2}$ and so decouple from the spin-$\frac{1}{2}$ channel to leave 8 coupled equations.

A very similar set of equations can be derived for spin-$\frac{3}{2}$ states. The kernel has the same form as given in Eq. (32); only the numerical coefficients differ from spin-$\frac{1}{2}$ case. From Eq. (26) we see that $C^{3/2}_{a'a}$ is equal to $+2$ if both indices refer to axial diquarks and zero otherwise. Since the components involving scalar diquarks do not contribute, the number of coupled equations is again reduced to 8.

V. NUMERICAL METHOD

We solve the Faddeev equation (31) in the rest frame of the nucleon (or Δ), where $P = (E, \vec{0})$. To avoid the singularities of the kernel, we perform a Wick rotation on the energy variables p_0 and p'_0: $p_0 \to \alpha + ip_4$ with

$$\alpha = \frac{M - m_{\rm diq}}{2}, \tag{35}$$

where $m_{\rm diq}$ is the lower-energy pole in the diquark T-matrices, (12) and (16) (i.e. the mass of the lighter diquark).

Because of the Wick rotation, we have to solve 8 complex coupled integral equations. We do so using the iterative method of Malfliet and Tjon [29,30]. The set of equations may be written schematically as

$$K(E)\Phi = \Phi, \tag{36}$$

where the kernel $K(E)$ depends nonlinearly on the energy eigenvalue E. Rather than solve this directly, we solve instead the linear eigenvalue problem

$$K(E)\Phi = \lambda(E)\Phi, \tag{37}$$

for a fixed value of E. This is done iteratively, by acting with $K(E)$ on some initial guess for the vector Φ of vertex functions to obtain a new vector. This is repeated until the vectors of functions in successive iterations are simply proportional to each other. The proportionality constant is then equal to $\lambda(E)$. We search on E until we find a value for which $\lambda(E) = 1$ and so the solution Φ satisfies the original equation (36). In the present problem, we use a

simple initial guess consisting of a Gaussian for the real part of each of the 8 components of Φ, and the derivative of a Gaussian for each of the imaginary parts. We find that 4 or 5 iterations are generally enough to determine $\lambda(E)$.

The parameters of the model that describe the interactions in the qq channels are fixed using the solutions to the Faddeev equation at zero density. The values of the scalar and axial-vector couplings g_S and g_A that reproduce the masses of the nucleon and the Δ are listed in Table I for our two parameter sets.

Before describing our calculations at finite density, we should compare our zero-density results with those in Ref. [18]. Note that apart from the difference in cut-off scheme and the use of current quark masses, a further difference between our approach and theirs is that Ishii *et al.* do not try to reproduce the nucleon and Δ masses exactly, but investigate the range of parameters g_S/g_π and g_A/g_π that can give bound states with reasonable masses. When only the scalar coupling is included ($g_A/g_\pi = 0$), we find that the minimum value of g_S/g_π to get a bound nucleon is 0.8 compared with 0.5 in Ref. [18], both for a quark mass of $M = 400$ MeV. Although these values are rather different, one should note that the nucleon is very weakly bound in the absence of the axial qq coupling. For example, Ishii *et al.* find a nucleon binding energy of only about 40 MeV for $g_S/g_\pi = 0.8$. It is therefore not too surprising that the point at which the nucleon becomes bound is rather sensitive to details, such as the choice of regulator or the use of the chiral limit.

With both scalar and axial couplings the nucleon is more strongly bound and one might hope that results are less sensitive, but in this case it is harder to make meaningful comparisons with the results of Ref. [18] because of the problem with the erroneous factor of 4 in the axial channel mentioned above. For a quark mass of $M = 420$ MeV we are able to fit the nucleon and Δ masses with $g_S/g_\pi = 0.735$ and $g_A/g_\pi = 0.33$. The value for the axial-vector coupling is smaller than the minimum value to bind the Δ of 0.44 in Ref. [18]. The value for the scalar coupling is rather somewhat larger than the range considered in that work. As in the case of the diquarks, there are indications that our approach tends to give less attraction in the scalar channel, compared with that of Ishii *et al.*, but more attraction in

the axial channel. Overall, though, the results are qualitatively similar.

The Faddeev equation at finite density is solved using the same methods. In this case the constituent quark mass is density dependent, and the 3-momentum of the valence quarks must be restricted to be larger than the Fermi momentum k_F. This acts as a lower cut-off of the momentum integrals: $k_F < |\mathbf{p}_i| < \Lambda$ for the three-momenta $\mathbf{p}_i$ of all three quarks. A similar Wick rotation is performed on the energy variables, but with

$$\alpha(k_F) = \frac{\sqrt{M(k_F)^2 + k_F^2} - E_{\rm diq}(k_F)}{2}, \tag{38}$$

where $E_{\rm diq}(k_F)$ is the lower-energy pole in the diquark T-matrices at finite density.

VI. RESULTS

We have solved the Faddeev equation at finite density for the energy E_N of a nucleon at rest. In Figs. 3(a) and 3(b) we show the binding energy of the nucleon B_N as a function of the Fermi momentum k_F for our two sets of parameters. For these parameter sets the scalar diquark is more strongly boundthan the axial, and so the nucleon binding energy is defined as

$$B_N = E_S + \sqrt{k_F^2 + M^2} - E_N, \tag{39}$$

with respect to the quark-diquark threshold. This is the relevant threshold since the NJL model does not exhibit confinement. We compare B_N to the binding energy of the scalar diquark

$$B_S = 2\sqrt{k_F^2 + M^2} - E_S. \tag{40}$$

The binding with respect to the three-quark threshold is given by the sum of B_N and B_S. One can see that the behaviors of the nucleon and the scalar diquark at finite density are quite different. The binding energy of the diquark is very large and initially tends to increase with density, only decreasing when the Fermi momentum approaches the cut-off. In contrast,

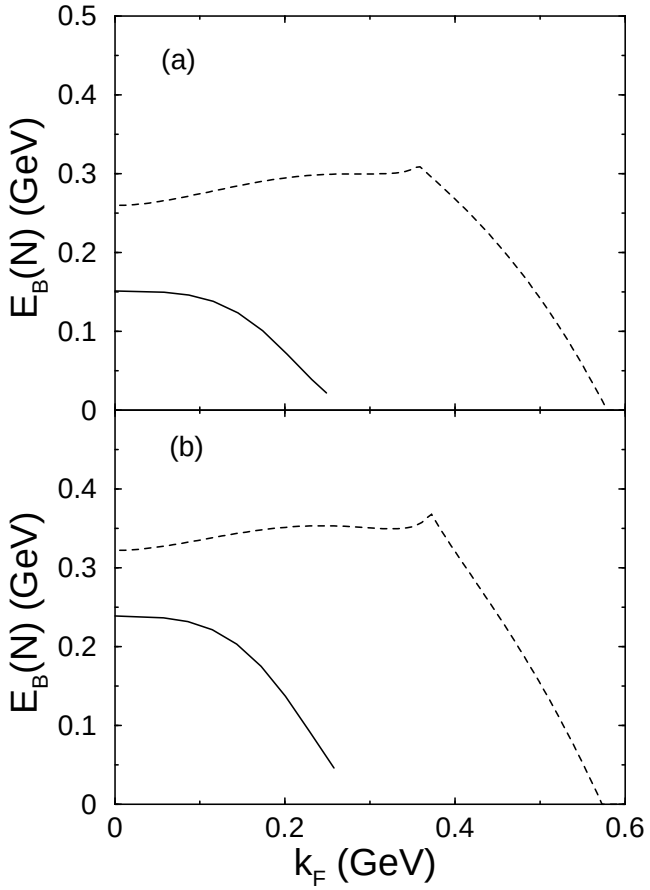

FIG. 3. The binding energy of the nucleon (continuous curve) and of the scalar diquark (dashed curve) as a function of k_F for the parameter sets with (a) $M = 450$ MeV and (b) $M = 500$ MeV.

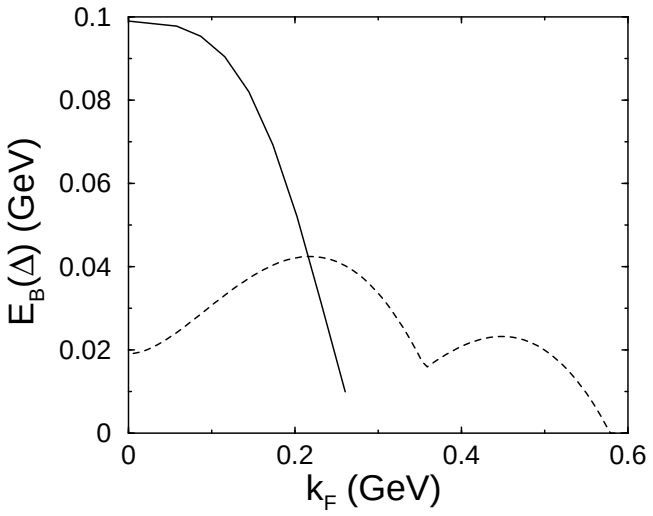

FIG. 4. The binding energy of the Δ (continuous curve) and of the axial-vector diquark (dashed curved) as a function of k_F for the parameter set with $M = 450$ MeV.

the binding of the nucleon decreases rather quickly, so that it is only marginally bound at nuclear matter density ($k_F = 270$ MeV).

We have also calculated the binding energy of the Δ as a function of k_F and this is shown in Fig. 4. In this case the threshold is determined by the binding energy of the axial diquark, which is also shown in Fig. 4. The behavior is similar to that found in the case of the nucleon. Since the axial coupling is smaller than the scalar coupling, the axial diquark is less strongly bound than the scalar one. Nonetheless it remains bound over the whole range of densities considered, while the Δ becomes unbound near nuclear matter density. Chiral symmetry restoration occurs at $k_F = 359$ MeV and $k_F = 372$ MeV for the parameter sets with $M = 450$ MeV and $M = 500$ MeV respectively, which corresponds to the cusps in the diquark binding in Figs. 3 and 4.

Another perspective can be gained by plotting the total energy of the nucleon instead of its binding energy, as is done in Fig. 5. For comparison, we have also plotted the quark-diquark threshold and the three-quark threshold. One can see that the nucleon energy increases only slightly with density, while the quark-diquark threshold decreases more and more quickly as one approaches the density of chiral restoration (which is basically a consequence of the vanishing of the constituent quark mass at the transition). The density

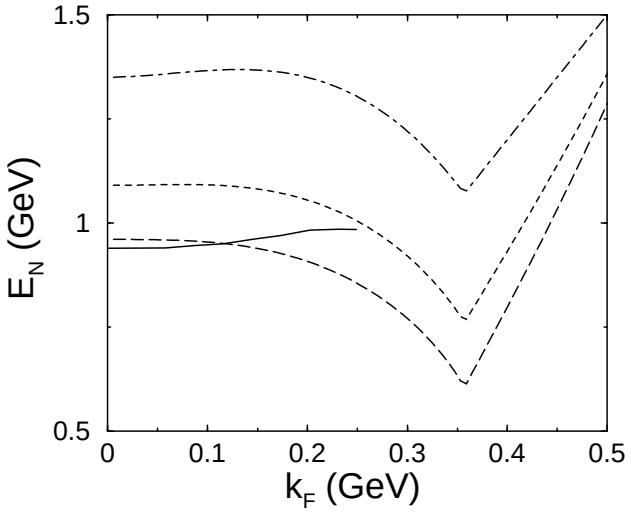

FIG. 5. The energy of the nucleon (continuous curve) as a function of k_F compared with 3/2 times the mass of the scalar diquark (long-dashed curve), the quark-diquark threshold (short-dashed curve) and the three-quark threshold (dash-dotted curve), for the parameter set with $M = 450$ MeV.

dependence of the Δ energy shows the same qualitative behavior.

To answer the question raised in the introduction about the possible competition between diquark and three-quark clustering, we have also plotted the quantity $\frac{3}{2}E_S$. If $E_N < \frac{3}{2}E_S$ then a system of six quarks will prefer to form two nucleons, while if $E_N > \frac{3}{2}E_S$ it will form three diquarks. Fig. 5 shows that nucleons are more stable than diquarks only for Fermi momenta smaller than about 130 MeV, which corresponds to 1/8 of nuclear matter density. For our other parameter set, with $M = 500$ MeV, nucleons remain more stable than diquarks up to $k_F = 170$ MeV, or 1/4 of nuclear matter density. These results clearly cast doubt on the validity of the model in this regime.

VII. CONCLUSIONS

We find that the NJL model predicts that, except well below nuclear matter density, it is energetically much more favorable to form three diquarks than it is to form two nucleons, and that there are no nucleon instabilities for the high densities where color superconductivity is expected to occur.

However we should not conclude on the basis of these results that there is no competition between nucleon formation and diquark condensation. Since this model predicts that nuclear matter should consist of diquarks, a result clearly at odds with what is actually observed, some elements of reality are missing. The most obvious of those is the lack of explicit confinement in the NJL model, something that is not easily remedied. It poses a rather deep question about the interpretation of the NJL model at finite densities. In much of the recent literature it has been used to model an instanton-induced interaction between the quarks in high-density matter beyond the chiral/deconfining phase transition. We have tried to follow a more traditional approach, where the model is interpreted as a density model for hadron structure in the vacuum. In that case the model contains *unphysical* diquark degrees of freedom, which may be ignored at zero density as being "irrelevant". Both of these approaches have flaws. In the first (high-density) interpretation, we have no clue as to what remnants of confinement may play a role in the interaction. In the second (low-density) interpretation we cannot even describe nuclear matter properly.

Standing back and looking at our results in the light of these problems with the model, we note from Fig. 5 that the nucleon energy is roughly independent of density. It is mainly the increase in the diquark binding that renders the nucleon unstable. One could naively add to the NJL model a three-body force that provides attraction in the color-singlet channel, to incorporate an approximate description of confinement. Alternatively one might modify our treatment to use confined rather than free quark and diquark propagators [20]. Both of these choices have some appeal, but neither really deals with the underlying mechanism of confinement.

One should also remember that our results have all been obtained using the "rainbow-ladder" approximation to the diquark Bethe-Salpeter equation and the Faddeev equation. In the context of models with nonlocal interactions between the quarks, it has been shown [31,32] that this approximation over-predicts diquark binding. With a toy model for the gluon propagator which leads to quark confinement, diquark condensation has been shown to occur even though diquarks are no longer bound at zero density [33]. Hence another way

to approach this problem may be to study the Faddeev equation within a less restrictive calculational scheme.

In conclusion, it is clear that the question of how confinement and the related three-quark correlations affect the phase structure of baryonic matter still remains to be answered.

ACKNOWLEDGMENTS

We are very grateful to Noriyoshi Ishii for providing us valuable details of the derivation of the Bethe-Salpeter and Faddeev equations. This work was supported by the EPSRC under grants GR/J95775 (Manchester) and GR/L22331 (UMIST).

REFERENCES

[1] I. Barbour, S. Morrison, E. Klepfish, J. Kogut, M.-P. Lombardo, Nucl. Phys. B, Proc. Suppl. **60A**, 220 (1998).

[2] M. Alford, A. Kapustin and F. Wilczek, Phys. Rev. D **59**, 054502 (1999).

[3] M. Alford, K. Rajagopal and F. Wilczek, Phys. Lett. B **422**, 247 (1998).

[4] R. Rapp, T. Schäfer, E. Shuryak and M. Velkovsky, Phys. Rev. Lett. **81**, 53 (1998).

[5] D. Bailin and A. Love, Phys. Rep. **107**, 325 (1984).

[6] M. Iwasaki and T. Iwado, Phys. Lett. B **350**, 163 (1995).

[7] J. Berges and K. Rajagopal, Nucl. Phys. **B538**, 215 (1999).

[8] D. I. Diakonov, H. Forkel and M. Lutz, Phys. Lett. B **373**, 147 (1996).

[9] T. Schwarz, S. Klevansky and G. Papp, Phys. Rev. C **60**, 055205 (1999).

[10] M. Alford, K. Rajagopal and F. Wilczek, Nucl. Phys. **A638**, 515c (1998).

[11] K. Rajagopal, hep-ph/9908360.

[12] T. Schäfer, nucl-th/9911017.

[13] M. Beyer, W. Schadow, C. Kuhrts and G. Röpke, Phys. Rev. C **60**, 034004 (1999).

[14] A. Buck, R. Alkofer and H. Reinhardt, Phys. Lett. B **286**, 29 (1992).

[15] N. Ishii, W. Bentz and K. Yazaki, Phys. Lett. B **318**, 26 (1993).

[16] H. Meyer, Phys. Lett. B **337**, 37 (1994).

[17] S. Huang and J. Tjon, Phys. Rev. C **49**, 1702 (1994).

[18] N. Ishii, W. Bentz and K. Yazaki, Nucl. Phys. **A587**, 617 (1995).

[19] C. Hanhart and S. Krewald, Phys. Lett. B **344**, 55 (1995).

[20] G. Hellstern, R. Alkofer, M. Oettel and H. Reinhardt, Nucl. Phys. **A627**, 679 (1997); M. Oettel, G. Hellstern, R. Alkofer and H. Reinhardt, Phys. Rev. C **58**, 2459 (1998).

[21] M. C. Birse, J. A. McGovern, S. Pepin and N. R. Walet, nucl-th/9905032.

[22] Y. Nambu and G. Jona-Lasinio, Phys. Rev. **122**, 345 (1961); **124**, 246 (1961).

[23] S. Klevansky, Rev. Mod. Phys. **64**, 649 (1992).

[24] T. Hatsuda and T. Kunihiro, Phys. Rep. **247**, 221 (1994).

[25] C. Itzykson and J.-B. Zuber, *Quantum Field Theory*, (McGraw-Hill, New York, 1980).

[26] N. Ishii, private communication.

[27] A. R. Edmonds, *Angular Momentum in Quantum Mechanics*, (Oxford University Press, Oxford, 1957).

[28] M. Jacob and G. C. Wick, Ann. Phys. **7**, 404 (1959).

[29] R. A. Malfliet and J. A. Tjon, Nucl. Phys. **A127**, 161 (1969).

[30] G. Rupp and J. A. Tjon, Phys. Rev. C **37**, 1729 (1988).

[31] A. Bender, C. D. Roberts and L. van Smekal, Phys. Lett. B **380**, 7 (1996).

[32] G. Hellstern, R. Alkofer and H. Reinhardt, Nucl. Phys. **A625**, 697 (1997).

[33] J. C. R. Bloch, C. D. Roberts and S. M. Schmidt, nucl-th/9907086.